colloids and interfaces

MDPI

Article

Utilizing TPGS for Optimizing Quercetin Nanoemulsion for Colon Cancer Cells Inhibition

Hadel A. Abo Enin [1,*], Ahad Fahd Alquthami [2,†], Ahad Mohammed Alwagdani [2,†], Lujain Mahmoud Yousef [2,†], Majd Safar Albuqami [2,†], Miad Abdulaziz Alharthi [2,†] and Hashem O. Alsaab [2,*]

1 Pharmaceutics Department, National Organization of Drug Control and Research (NODCAR), Giza P.O. Box 12511, Egypt
2 Department of Pharmaceutics and Pharmaceutical Technology, College of Pharmacy, Taif University, P.O. Box 11099, Taif 21944, Saudi Arabia
* Correspondence: hadelaboenin@outlook.com (H.A.A.E.); h.alsaab@tu.edu.sa (H.O.A.); Tel.: +966-556-047-523 (H.O.A.)
† These authors contributed equally to this work.

Abstract: *Background:* Colorectal cancer is one of the most challenging cancers to treat. Exploring novel therapeutic strategies is necessary to overcome drug resistance and improve patient outcomes. Quercetin (QR) is a polyphenolic lipophilic compound that was chosen due to its colorectal anticancer activity. Nanoparticles could improve cancer therapy via tumor targeting by utilizing D-tocopheryl polyethylene glycol succinate (vitamin-E TPGS) as a surfactant in a nanoemulsion preparation, which is considered an efficient drug delivery system for enhancing lipophilic antineoplastic agents. Thus, this study aims to develop and optimize QR-loaded nanoemulsions (NE) using TPGS as a surfactant to enhance the QR antitumor activity. *Method:* The NE was prepared using a self-assembly technique using the chosen oils according to QR maximum solubility and TPGS as a surfactant. The prepared QR-NE was evaluated according to its particle morphology and pH. QR entrapment efficiency and QR in vitro drug release rate were determined from the selected QR-NE then we measured the QR-NE stability. The anticancer activity of the best-selected formula was studied on HT-29 and HCT-116 cell lines. *Results:* Oleic acid was chosen to prepare QR-NE as it has the best QR solubility. The prepared NE, which had particles size < 200 nm, maximum entrapment efficiency > 80%, and pH 3.688 + 0.102 was selected as the optimal formula. It was a physically stable formula. The prepared QR-NE enhanced the QR release rate (84.52 ± 0.71%) compared to the free drug. QR-NPs significantly improved the cellular killing efficiency in HCT-116 and HT-29 colon cancer cell lines (lower IC50, two folds more than free drug). *Conclusion:* The prepared QR-NE could be a promising stable formula for improving QR release rate and anticancer activity.

Keywords: colorectal cancer; nanoemulsion; quercetin; TPGS; drug delivery system

Citation: Enin, H.A.A.; Alquthami, A.F.; Alwagdani, A.M.; Yousef, L.M.; Albuqami, M.S.; Alharthi, M.A.; Alsaab, H.O. Utilizing TPGS for Optimizing Quercetin Nanoemulsion for Colon Cancer Cells Inhibition. *Colloids Interfaces* **2022**, *6*, 49. https://doi.org/10.3390/colloids6030049

Academic Editors: César Burgos-Díaz, Mauricio Opazo-Navarrete and Eduardo Morales

Received: 26 July 2022
Accepted: 2 September 2022
Published: 19 September 2022

1. Introduction

Colorectal cancer is one of the most common cancers in men and the third among women globally. More than 1.9 million new colorectal cancer cases and 935,000 deaths were estimated to have occurred in 2020 [1,2]. Although its mortality rates have decreased in all populations, the American Indians and Alaskan natives still suffer mostly at a high rate [3,4]. Nowadays, newer applications are used to diagnose and treat colorectal cancer due to their excellent enhancement of conventional methods and the development of novel approaches for detection and therapy, such as nanotechnology [5–7]. Recent nanotechnologies applications in colorectal cancer therapy have utilized nano-sized particle (NP)-based specific delivery systems for enhancing chemo and targeted therapy for tumors. These novel treatment approaches enhance drug permeability and drug retention effect [8,9]. The enhancing permeability and retention (EPR) effect arises from the leaky vasculature and impaired lymphatic drainage in the tumor cells [10,11].

Tumor targeting is one of the main nanotechnology advantages in cancer treatment. A NPs drug delivery system could improve drug delivery to malignant cells with less accumulation in nonmalignant cells [12]. This could be achieved by passive and/or active targeting, for targeting malignant and nonmalignant cells. In passive targeting, nano-drug particles could entrap the tumor cells, which could enhance the permeability and retention (EPR) [13]. To localize nano-drug particles to cancer cells, active targeting is promising, using selective molecular recognition as antigens or frequently expressed proteins on the surfaces of cancer cells. It also takes advantage of biochemical properties associated with cancer, such as matrix metalloproteinase secretion [14].

Nanoscale drug delivery systems, commonly referred to as nanocarriers, are nano-sized materials that can carry multiple drugs or imaging agents. Nanoemulsions (NE) as nanoscale delivery systems can deliver hydrophobic cytotoxic antineoplastic drugs with efficient pharmacokinetics and pharmacodynamics patterns. NE can also enhance the dose efficacy, reduce the drugs' side effects, increase the drug surface area, ease preparation, improve the thermodynamic stability, and help target and sustain controlled drug delivery [15–17].

Quercetin (QR) is a bioactive flavonoid compound (flavanol class) with strong anti-cancer activity besides its anti-inflammatory, anti-oxidant, and vasodilator effects [18,19]. QR anticancer activity works by adjusting cell-cycle progression, promoting apoptosis by reducing the expression stage of anti-apoptotic proteins, inhibiting angiogenesis and metastasis progression, affecting autophagy, and inhibiting cell proliferation [19,20]. According to its rapid clearance and lower water solubility and stability, the lower QR's oral bioavailability and high therapeutic dose (about 500 mg twice daily) are the primary oral QR limitations [21]. QR stability changes in a physiological medium as it is affected by pH, temperature, and oxidation [21]. In addition, using D-tocopheryl polyethylene glycol succinate (vitamin E TPGS) surfactant in nanocarrier is promising. TPGS is the water-soluble derivative of vitamin E. It contains a hydrophilic polar head and the lipophilic alkyl tail, which has been shown to have beneficial effects on the solubilization of QR, inhibiting P-gp mediated by hindering P-gp efflux on intestinal brush borders. TPGS has proved its essential role in chemotherapy by inducing cell-cycle arrest, promoting apoptosis, and enhancing permeation in the cancer cell [22]. Therefore, in this study, QR will be loaded in NPs as a NE formulation using TPGS as a surfactant to overcome the QR drawbacks and enhance its antitumor efficacy.

2. Materials and Methods

2.1. Materials and Cell Lines

The QR, medium-chain triglyceride, glyceryl monooleate (GMO), oleic acid, PEG 400, and surfactants (TPGS) were bought from Sigma-Aldrich Co (St. Louis, MO, USA). Colon cancer cell lines HCT-116 and HT-29 ATCC® were taken from our collaborator and were cultured in Gibco DMEM (Dulbecco's modified Eagle's medium) containing 4.5 g of glucose/liter (Thermofisher Scientific, Waltham, MA, USA) and including 10% fetal bovine serum (FBS; Thermo Fisher Scientific, Waltham, MA, USA). For MTT studies, the cell culture media were maintained at 37 °C and 5% CO_2 after being supplemented with 100 units/mL of penicillin and 100 µg/mL of streptomycin.

2.2. Selection of the Oil Phase

The appropriate oil for NE formulation is the oil improving the drug solubility to increase the drug-entrapping efficiency. An excess QR amount was separately added to 5 mL of certain oils such as MCT, glyceryl monooleate (GMO), and oleic acid (all of the above vehicles were in a liquid phase at 37 °C) for 72 h to achieve a dissolution equilibrium state. The samples were centrifuged at 10,000 rpm for 10 min. The QR concentrations in the supernatant were quantified by UV analysis at 370 nm using Synergy 2 UV Microplate Reader by BioTek Instruments, Inc. The solubility result was the mean of three experiments ± SD [23].

2.3. Preparation of Quercetin-Loaded NEs (QR-NEs)

QR-NE was prepared by the high-pressure homogenization (HPH) method, as described previously by Sessa et al. [24]. The emulsion components were selected based on several preliminary trials, and the chosen oil was the oil that had the maximum drug solubility. Oil phase (the selected oil) 10 w/w% was heated at 70 °C, then 0.1 w/w% QR was added and magnetically stirred for 15 min, till complete drug solubilization. The aqueous phase consists of distilled water containing 8 w/w% surfactants (TPGS) heated to the same temperature as the oil phase. Coarse emulsions were prepared by adding the oil phase into the aqueous phase under magnetic stirring at 500 rpm for 10 min. The coarse emulsions were passed through a high-pressure homogenizer to obtain final NE (AH100D, ATS Engineering, BVI, Canada), further dispersed by high-speed stirring using Ultra-Turrax (FM200, FLUKO Technology, Saarbrücken, Germany) at different homogenization rates (10,000, 12,000, 15,000) rpm for different times (10, 12, 15 min). To investigate the impacts of each independent variable (homogenizer speed and rotation time) and their combined effect on dependent variables (particle size and entrapment efficiency) one-way ANOVA was used with consideration of significant difference at $p < 0.05$ using Design Expert 7.0.0 Stat Ease. Inc. Minneapolis, MN, software [25].

2.4. Evaluation of the Prepared QR-NE

2.4.1. Nanoemulsion Particle Morphology

NE droplet size and zeta potential was determined by a Zeta-sizer (Zeta-sizer Ver. 7.01, Malvern Instruments). Separately, 0.1 mL of the prepared QR-NE formulation was dispersed in 50 mL of water and mixed well, and monitored at 25 °C ± 1.

2.4.2. Determination of Entrapment Efficiency

Entrapment efficiency (EE%) and loading capacity were determined by difference according to the following equations, respectively:

$$\text{EE (\%)} = \text{Weight of total drug in the formulation} - \text{Weight of drug in the aqueous phase (un-entrapped)} \times 100/\text{Weight of total drug in the formulation.} \quad (1)$$

$$\text{Drug loading (\%)} = (\text{Total weight of the drug}/\text{Total weight of sample}) \times 100\%. \quad (2)$$

The free drug concentration (un-entrapped) was determined in the supernatant after centrifugation of the prepared QR-NE formulations at 13,300 rpm and 4 °C for 60 min (Eppendorf, Hamburg, Germany). The QR amount in the supernatant was assessed against a blank (free QR formulation we prepared and treated under the same conditions) using a UV spectrophotometer (Pharmacia/Amersham Ultrospec 4000 UV/VIS Spectrophotometer) at 370 nm [26].

2.4.3. Determination of pH

The pH of the formulation was measured using a digital pH meter (Metler Toledo, OH, USA). Results were taken as the mean ± SD of three measures to reduce the error. pH is an important parameter as mainly the used excipients in the formulation decide the pH of the final preparation and hence the route of administration.

2.5. Studying the Physical Stability of QR-NE

2.5.1. Centrifugation Method

The selected formula was centrifuged at 5000 rpm for 10 min to check its physical stability. The nanoemulsion system was observed visually for the appearance of any creaming or phase separation [27].

2.5.2. Agitation Test

Three grams of QR-NE selected formula were accurately weighed and placed in a petri dish on a platform shaker at 50 rpm for 24 h at room temperature using an orbital shaker. The sample was observed for signs of any cream or oil droplets (phase separation) [28].

2.5.3. Heating Cooling Cycle

The formulae were stored between refrigerator temperatures 4 °C and 45 °C for six cycles with storage at each temperature and not less than 48 h. The formulations, stable at these temperatures, were subjected to centrifugation [29].

2.6. In Vitro Drug Release Study of QR from QR-NEs

The in vitro release study was conducted separately on free drug (QR) suspension and the selected formula (QR-NE). Two grams from each, separately, were put in a dialysis bag (molecular weight cut-off 3500). The dialysis bags were put into a beaker containing 50 mL of the release medium at 37 °C and mechanically stirred at 100 rpm. At specific time intervals, 2 mL release medium (10% alcoholic water; to maintain a sink condition) was withdrawn and replaced with an equivalent fresh medium. QR-released concentration was determined using a UV-spectrophotometer. Three independent experiments were conducted, and the data were expressed as mean ± SD [30].

2.7. Transmission Electron Microscopy (TEM)

For morphology, transmission electron microscopy (TEM) characterization of the tested selected formula was tested using the JEOL JEM-1000 instrument (JEOL Ltd., Tokyo, Japan). Fifty microliters of the selected sample were placed on a film-coated 200-mesh copper specimen grid for 10 min, and the fluid excess was eliminated using filter paper. The prepared grid was stained using 3% phosphotungstic acid (one drop) and dried for 3 min. The dried sample was examined using the TEM microscope (Philips, CM 12). The sample was observed by operating at 120 kV.

2.8. Evaluation of the Anticancer Activity against HT-29 and HCT-116 Cells

The cytotoxicity of the selected QR-NE formula was studied on HT-29 and HCT-116 cells using MTT-colorimetric method. An MTT assay was used to evaluate the viability of cancer cell lines following 48 h of treatment with quercetin at 5, 10, 20, 50, and 100 μM. Free QR was used as a control. Both cells were seeded in 96-well plates at a density of 5×10^3 cells and then incubated for 24 h. Subsequently, the cells were treated with series concentrations of free QR and the selected formula of QR-NE (containing an equivalent concentration of QR) separately for 24 h. The cell viability was evaluated with MTT on a Synergy 2 Multi-Detection Microplate Reader by BioTek Instruments, Inc at 570 nm. The inhibitory concentration (50%) was determined from 3 independent experiments conducted, and the result was expressed as mean ± standard deviation compared to full proliferation (100%), which was obtained from untreated cells and was considered a negative control [31].

2.9. Animals' Treatment and Histological Analysis of Tissues after QR-NE Treatment

To evaluate the safety of QR-NE, male Wistar rats (200 ± 20 g) were used. The study was conducted according to the guidelines of the Declaration of Helsinki and approved by the Institutional Animal Care and Use Committee at Taif University, Taif, Saudi Arabia. The protocol number is (42-0112). The rats were kept and housed in the animal facility within optimal conditions (a quiet, stress-free, temperature-controlled environment, on a 12-h light/dark cycle). After housing for about a week in the laboratory conditions, the rats were randomly distributed into 3 groups (4 rats per group). Group (I): vehicle group (the rats were intraperitoneally treated with 1 mL/kg of normal saline); Group (II): free drug (the rats were intraperitoneally injected with 50 mg/kg of QR treatment); Groups (III): QR-NE treatment (the rats were intraperitoneally injected with 50 mg/kg of QR-NE treatment). All the treatments were continued for 5 consecutive days. Then, for evaluating

the effects of the compounds, the 12 h fasted rats were sacrificed by anesthetizing and both whole blood and the tissues were collected. For histopathological examination, a part of the collected tissues was fixed in 10% neutral buffered formalin. The histopathological alterations were assessed using the extracted specimens from liver, kidney, and spleen. The specimens were instantaneously fixed after being extracted in 10% formaldehyde and embedded in paraffin wax. Sections from specimens were slided (3–4 µm) after being deparaffinized and hydrated in distilled water. Then the sections were stained with hematoxylin and eosin (H&E) according to standard protocols to evaluate tissue architecture. Finally, histological images were taken using an inverted fluorescence microscope (Leica DMI8, Leica, Wetzlar, Germany).

2.10. Statistical Analysis

The results of in vitro and anticancer activity studies were expressed as the mean of three replicates ± SD. The paired t-test was used to compare two variables, while one-way ANOVA was used to assess the difference between groups using Design Expert 7.0.0 Stat Ease. Inc. software at a probability level $p < 0.05$ for significant differences. Sigmoidal concentration–response curve-fitting models and best-fit straight lines were used by Sigma plot software to calculate cell viability and cellular apoptosis, respectively. Cell viability was expressed as a percentage of survival compared to untreated cells, whereas cellular apoptosis was represented in folds compared to untreated cells (negative control).

3. Results and Discussion

3.1. The Selection of Oils

Different oils (GMO, medium-chain triglyceride, and oleic acid) were chosen as excipients due to their biocompatibility and low toxicity. Moreover, they have also been reported to form stable nanoemulsions without precipitation. As shown in Figure 1a, the solubility of QR was found to be highest in the oleic acid (18 carbon chain) [32]. Hence, the oleic was chosen as an oil phase to prepare nanoemulsion containing QR in this study ($p < 0.05$).

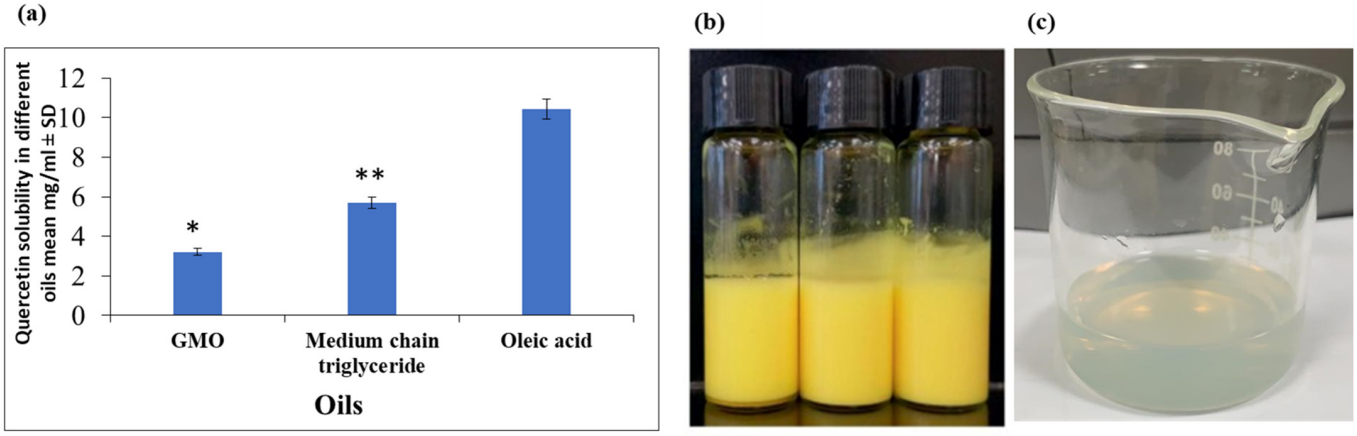

Figure 1. (**a**) Selection of oil for QR-NE preparation (there is a significant difference between GMO and MCT solubility results from oleic acid's results at $p = 0.068$ * and 0.041 **, respectively). (**b**) Quercetin emulsion using the selected oil (the composition as in the methods section). (**c**) Quercetin nanoemulsion after homogenization.

The NE preparations were mainly affected by their components. A preliminary study was conducted; the accepted formula was only the official formula considering the NEs have a homogenous yellow milky-like consistency. After homogenization treatments, stable, clear, and homogenous with no oil droplets solutions were obtained as shown in Figure 1b,c. Table 1 summarizes the nine experiment runs by studying the independent variables on the accepted particle size, DL, and EE%. As presented in Table 1, all formulations have an average particle size in the nano-range ranging from 9.522–273 nm. The drug-loading

content and encapsulation efficiency of the QR-NE can be measured compared to a standard curve. In this study, we obtained enough drug-loading ranging from 46.87% to 53.65%. As observed, increasing the homogenization speed led to decreasing the particle size as observed from the formulae from one to six, and a further increase in the homogenization speed of 15,000 rpm led to a further increase in the particle size as observed in the formulae from 7 to 9. This may be because either the droplet breakup was not continuous due to turbulent–inertial forces appearing in the used homogenizer, or there was retardation of droplet breakup or significant re-coalescence at higher pressures. These results agreed with previously reported results by Jafari et al. [33].

Table 1. Formulation parameters affect the particle size and entrapment efficiency.

PN	Speed (rpm)	Time (Min)	EE%	DL	PS (nm)
1	10,000	10	87.3 ± 2.5	46.87%	273.9 ± 2.22
2	10,000	12	91.2 ± 2.12	48.97%	127.7 ± 1.14
3	10,000	15	93.2 ± 1.87	51.84%	203.2 ± 1.98
4	12,000	10	83.5 ± 1.09	53.65%	50.59 ± 0.56
5	12,000	12	85.5 ± 1.11	50.98%	9.522 ± 0.11
6	12,000	15	88.9 ± 2.01	52.115	62.37 ± 0.87
7	15,000	10	79.1 ± 1.76	47.87%	155.3 ± 1.53
8	15,000	12	78.8 ± 1.65	49.97%	85.6 ± 0.16
9	15,000	15	77.1 ± 1.23	50.84%	105.2 ± 0.54

Abbreviations: PN: Patch number; EE%: Encapsulation efficiency; DL: Drug loading; PS: Particle size.

Also, Figure 2 illustrates the influence of homogenization speed and time on particle size. The following equation shows the effect of the different variables on QR-NEs particle size:

$$PS = 357.543362573099 - 0.0139235087719298 \times Speed - 5.39640350877193 \times Time. \quad (3)$$

The expressed equation (Equation (3)) revealed that the negative sign of the speed and time coefficients indicated a significant inverse relationship between the speed and time of homogenization and the particle size. The *p*-value for homogenization speed was 0.0368 ($p < 0.05$) which indicates that increasing the homogenization speed had a significant effect on particle size reduction while homogenization time has no significant effect on decreasing particle size; *p*-value = 0.0714 ($p > 0.05$). This could be due to increasing homogenization speed, which could amplify mechanical and hydraulic shear that breaks the emulsion gel structure into NE vesicles with a smaller particle size [34]. To be more precise, increasing the homogenization speed (from 10,000 rpm to 12,000 rpm) and homogenization time (from 10 min to 12 min) led to a decrease in the PS of the nanoemulsion formulations. Further increases resulted in a significant increase in particle size.

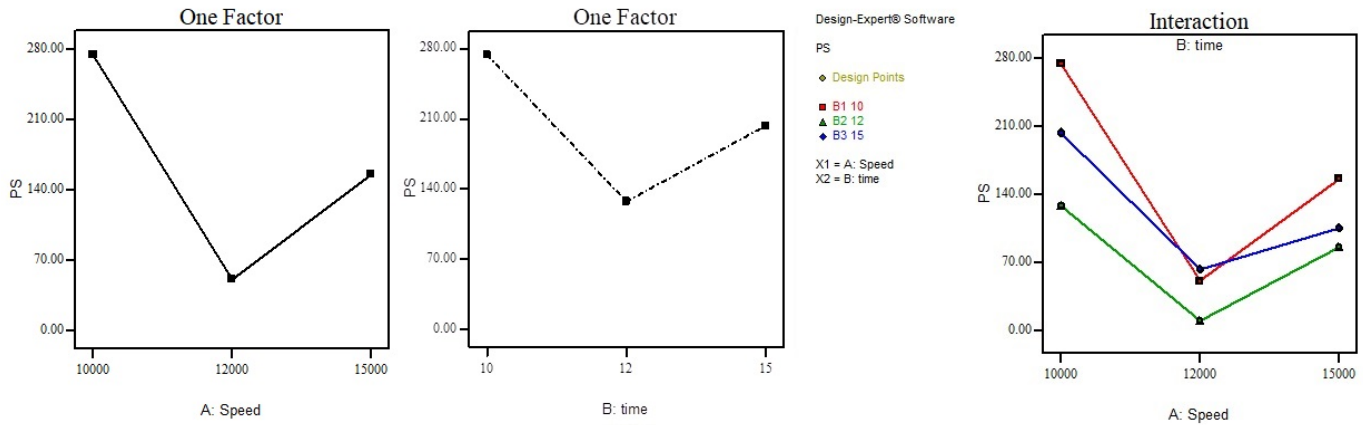

Figure 2. Effect of homogenization speed and time on the particle size (PS).

The effect of different formulation variables on EE% is noted in Table 1 and Figure 3. As noted in the following equation:

$$EE = 96.166081871345 - 0.0023140350877193 \times \text{Speed} + 0.612280701754387 \times \text{Time}. \quad (4)$$

The negative sign of homogenization speed indicates a significant antagonistic effect on EE% ($p < 0.05$). Increasing homogenization speed decreases the entrapping of QR into NE particles by reducing their contact. In contrast, a significant direct relation between homogenization time and EE% could be observed ($p < 0.05$). By increasing the contact time between drug and NE components, therefore EE% could be improved. This result agreed with previously reported works [35].

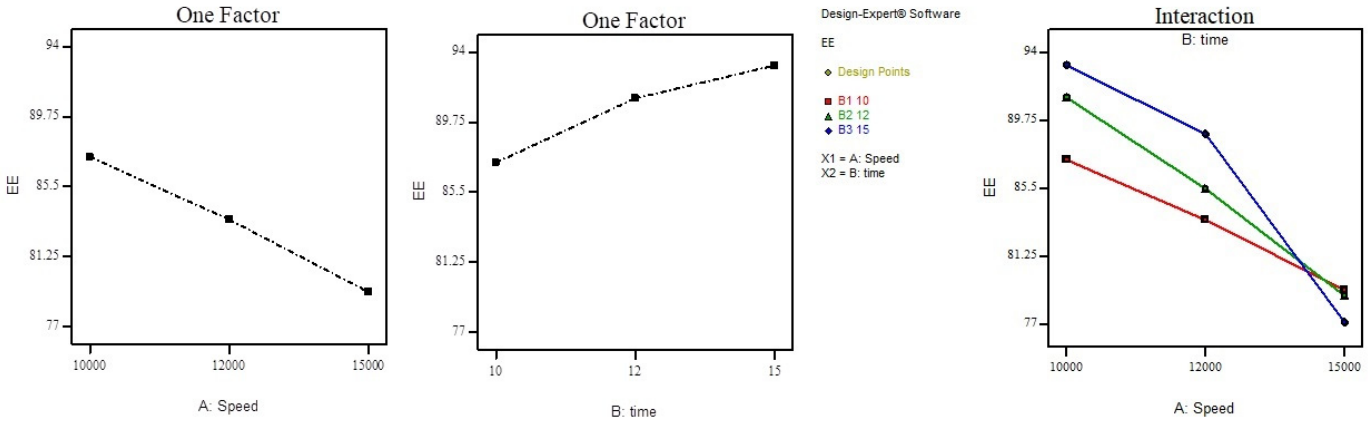

Figure 3. Effect of homogenization speed and time on the entrapping efficiency (EE).

3.2. Optimized QR-NE Formula Selection: Morphology and pH Determination

For formula optimization, the formulae with PS < 200 nm, higher DL > 50%, and maximum EE > 80% had higher priority and were chosen for further study. Therefore, formulae (F4, F5, F6) were selected. A paired t-test was applied to these formulae's PS and EE in pairs, and it was found that there were no significant differences between these formulae in the EE% results, while there was a substantial difference in the PS results. Therefore, F5 was chosen as it had a high EE% value, 85.5%, and the uniformly smallest PS with a high intensity of 96%, as represented in Figure 4a.

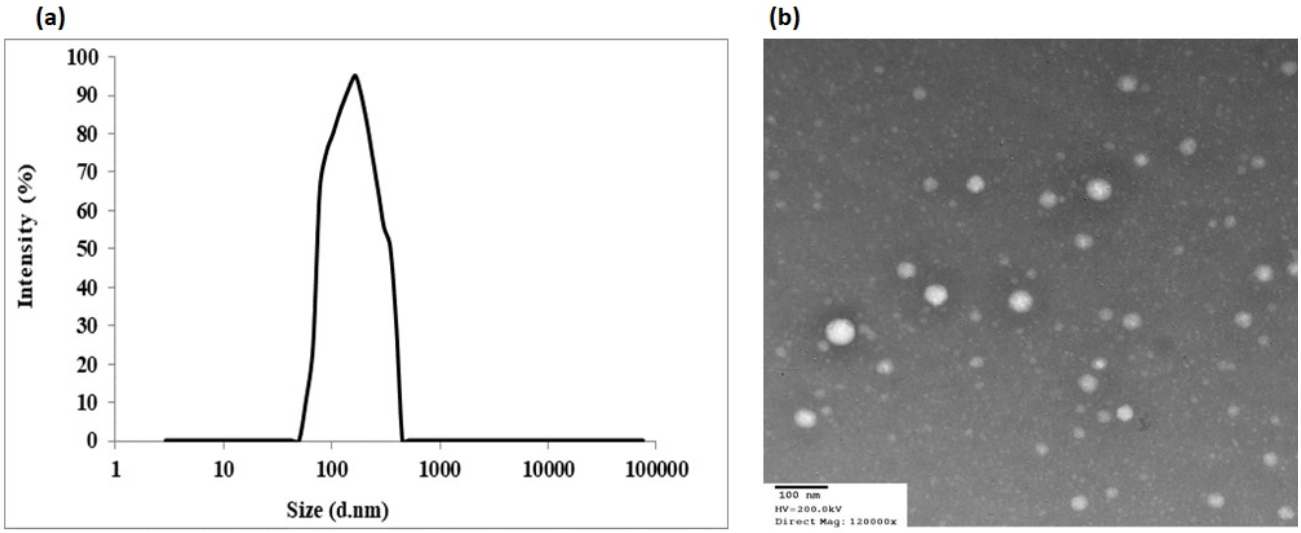

Figure 4. (**a**) Particle size distribution of QR-NE formula (F5). (**b**) QR-NEs (F5) Morphology under transmission electron microscopy (TEM) (magnification × 120,000).

Transmission electron microscopy characterization of F5 in Figure 4b shows that the nanoemulsion particles are uniformly nano-sized and have a spherical shape with a smooth and flexible boundary. No aggregation appears between the nanoparticles, indicating their stability against Ostwald ripening due to globular collapse [2]. This result agreed with previously reported results that TPGS could form a smooth particle layer, protecting the NE particles from severe structural changes.

The pH of the selected formula (F5) was 3.688 ± 0.102. The result indicates the suitability for oral administration of the prepared emulsion as it is closer to the stomach pH range (1.5–4). In addition, it is also more comparable to the large intestine pH (4–7); therefore, QR-NEs are suitable for colon administration [36].

3.3. Studying the Physical Stability of QR-NEs

After agitation and centrifugation on QR-NE (F5), there was no phase separation or creamy appearance in the prepared QR-NE formula. Nanoemulsion is a physically stable form of the prepared emulsion. In general, the nanoemulsion particles exhibit Brownian movement; therefore, no coalescence of droplets could occur except in the absence of this Brownian movement [37]. Centrifugation and agitation could contribute to the energy with which the NE droplets impinge upon each other. The lack of phase separation and creamy appearance after agitation and centrifugation indicates that QR-NE has good stability and can withstand the gravitational and mechanical forces during transportation and handling.

3.4. In Vitro Drug Release Study of QR from QR-NPs

The release results of the best-selected sample (QR-NE-F5) were compared in this respect with the release of free drug (QR). The release values were calculated as the percentage of QR dissolute according to the predetermined yield value. As noted in Figure 5, the QR-NPs showed an excellent release rate compared to free QR release. At the end of the release time (4 h), 25.63 ± 1.12% of free QR was released, which was considerably lower ($p < 0.05$) than released from QR-NE-F5 (84.52 ± 0.71%). The nanoemulsion formula's higher release rate can be attributed to its smaller particle size, which increases the surface area for diffusion. In general, NE is an excellent tool for enhancing the solubility of hydrophobic drugs such as QR; thereby, the bioavailability of the drug owing to small-scale globule size is improved. The presence of TPGS in NE can be attributed to the surfactant nature of TPGS, which enhances the QR release rate via increasing QR solubility [38,39]. TPGS as a surface active agent could improve drug wettability in contact with drug release media by adsorption on a larger surface area of nanoparticles and rapid drug partitioning into diluted dissolution medium, primarily from small droplets [40]. The TPGS layer around the QR NPs could protect the drug against gastrointestinal degradation, following which intestinal absorption would be further improved.

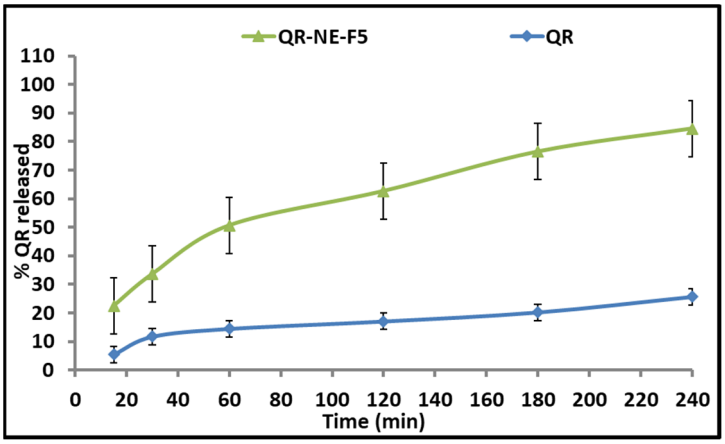

Figure 5. The cumulative released amount of quercetin (QR) and the selected formula (QR-NE-F5).

Many studies have concluded results in agreement with our results, which show that NE formulations usually result in an enhanced hydrophobic drugs release rate due to the effect of oil and interfacial film barriers [40,41].

3.5. Anticancer Activity of QR-NE; Cytotoxicity Study against Colorectal Cancer Cells

An MTT assay was used to evaluate the viability of HCT-116 and HT-29 colon cancer cell lines following 48 h of treatment with quercetin at 5, 10, 20, 50, and 100 µM. QR-NE inhibited CRC cell viability in a dose-dependent manner, which was more effective than the free drug. An increase in the concentration enhanced the viability of all cancer cell lines. More than twofold lower IC50 value of QR-NE (around 18 µM) indicates the superior anticancer effect of nanoparticle-based formulations on HCT-116 colon cancer cell lines, as shown in Figure 6a. We also found that the NE significantly improved the cellular killing in HT-29 colon cancer cell lines (around 15 µM) compared with the free drug, as shown in Figure 6b. Furthermore, the higher release rate of the QR combined with the lipid structure effect of the nanoemulsion increases drug concentration in colon cancer cells, improving the anticancer activity of the QR-NE formulations compared to free drug [41].

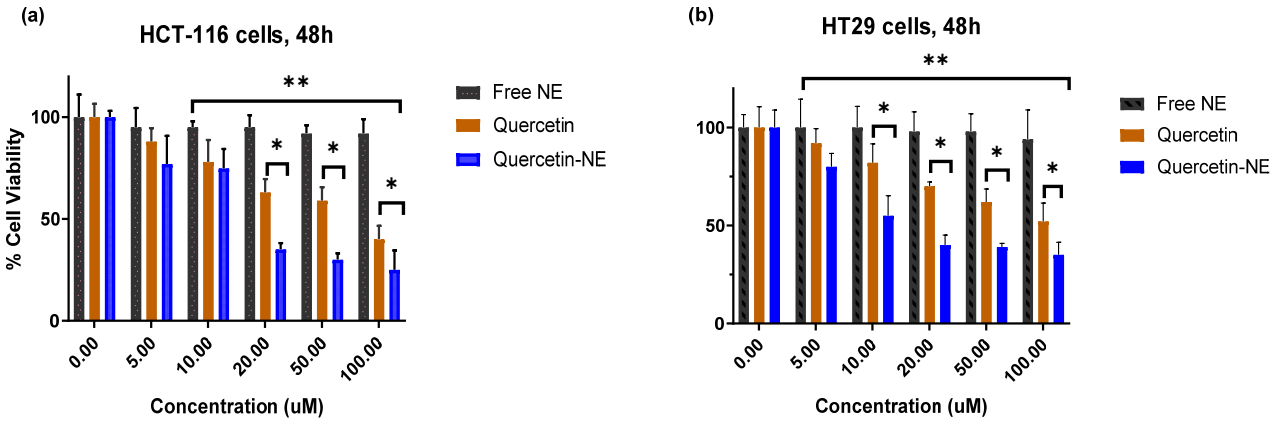

Figure 6. Cell viability of QR anticancer drug treated with 5–100 µM QR, QR-NE, and free NE up to 48 h for (**a**) HCT-116 and (**b**) HT-29 colon cancer cell lines. Results indicated that formulation inhibited CRC cell viability in a dose-dependent manner of QR-NE compared to free drugs, while empty NPs are nontoxic. The twofold lower IC50 value of QR-NE indicates the superior anticancer effect of nanoparticle-based formulations. Results are expressed as mean ± SD (n = 3). * $p < 0.01$, ** $p < 0.001$ based on two-way ANOVA followed by Sidak's multiple comparisons test.

3.6. QR-NE Safety Evaluation on the Animal Model

Macroscopic examination of all organs, including the liver, spleen, kidney, heart, lung, and brain tissue, revealed no differences 5 days after QR-NE (50 mg/kg) administration compared to organs of control rats which were treated with free NE and vehicle. There were no signs of atrophy, hyperplasia, necrosis, or inflammation.

To investigate tissue abnormalities, histological examination was performed using hematoxylin–eosin staining. For liver tissues, when compared to the control group, rats treated with QR-NE experienced no adverse effects on the liver. The parenchymal architecture revealed normal hepatocytes with no evidence of steatosis, inflammation, or fibrosis (Figure 7). Similarly, as shown in Figure 7, microscopic examination of the kidney, spleen, and heart revealed no evidence of inflammation or fibrosis. The histological sections of rats' liver, kidney, spleen, and heart are normal. Based on all gathered data, indications point to the safety of utilizing this nanoformulation for future efficacy studies.

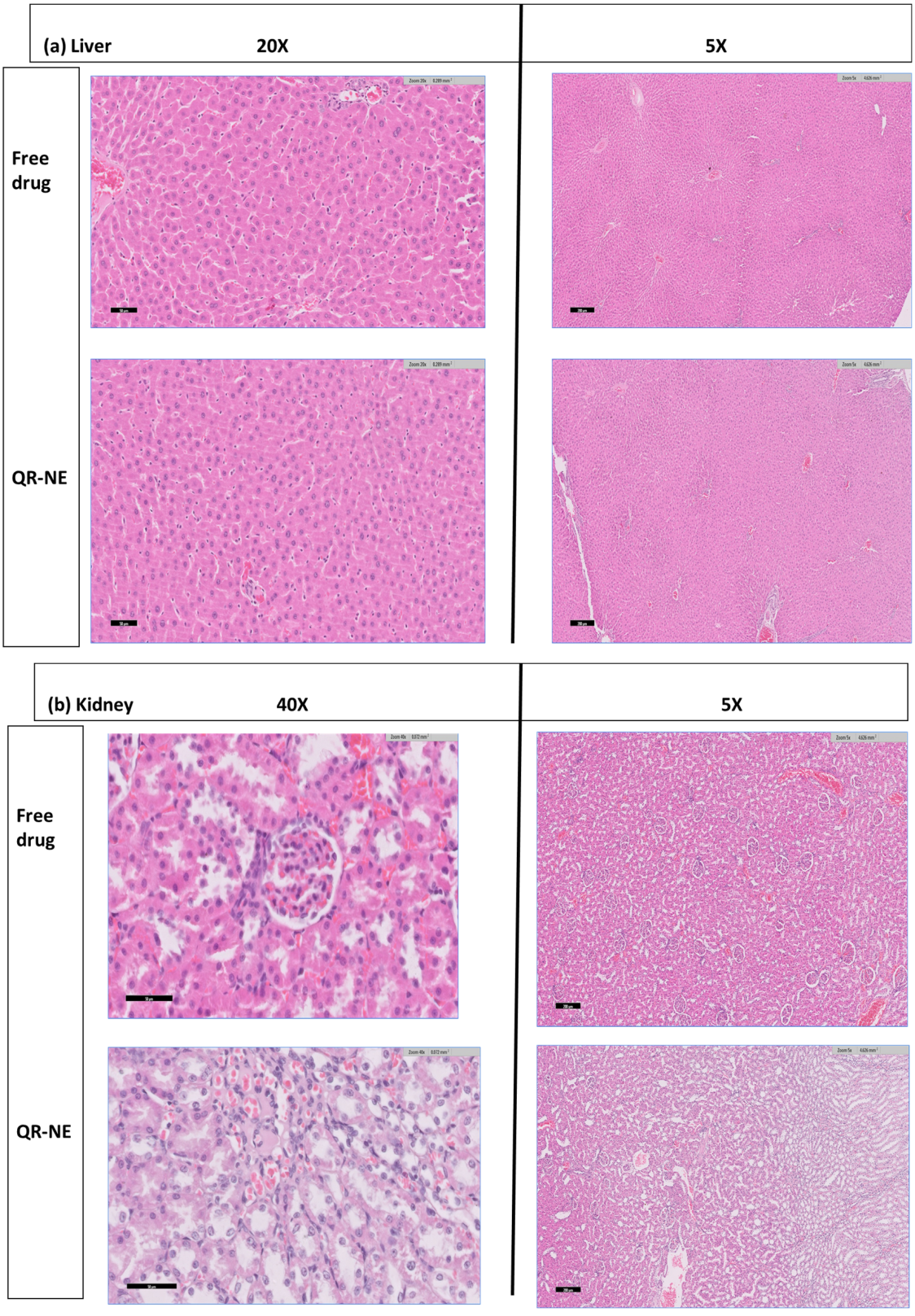

Figure 7. *Cont.*

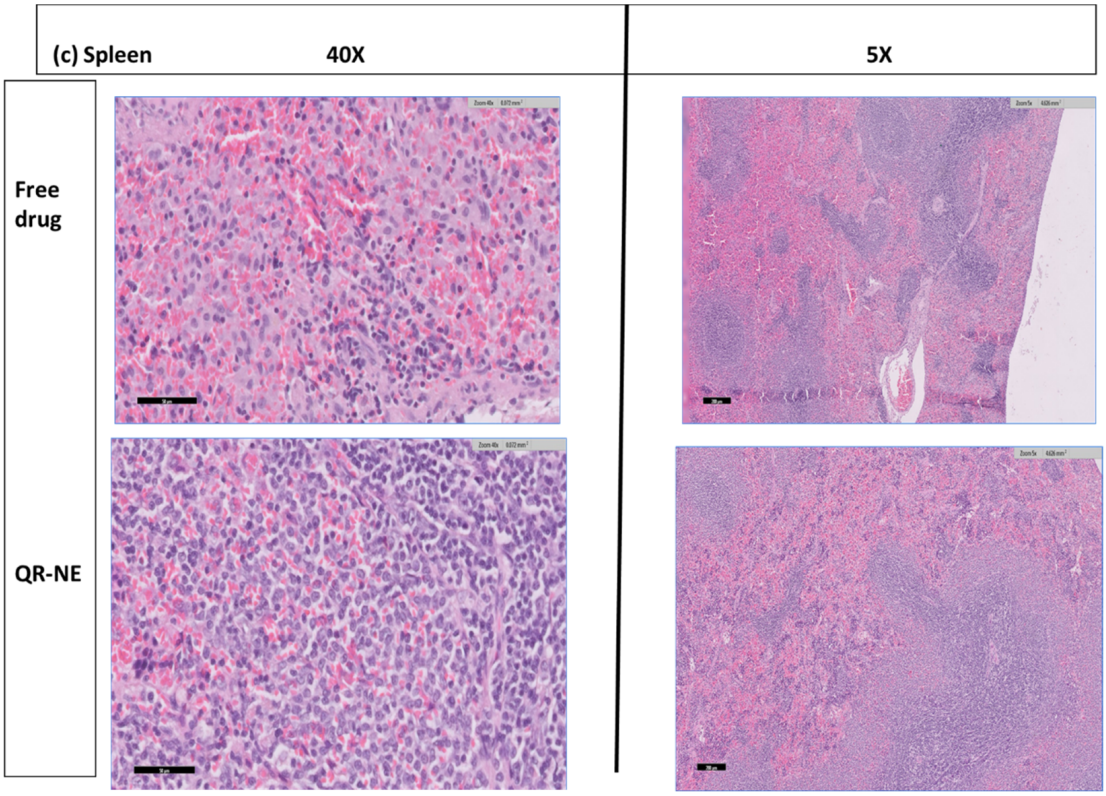

Figure 7. QR-NE safety evaluation on the animal model. Photomicrographs of (**a**) liver, (**b**) kidney, and (**c**) spleen sections after treatment with QR-NE and QR-free drug (H&E staining, magnification 40×, scale bar: 20 μm and 5×, scale bar: 200 μm). H&E hematoxylin and eosin sections were all treated with quercetin NE after 14 days. Histological evaluation was performed by ImageJ software version 1.52v.

4. Conclusions

The present study describes the development and safety of the QR-NE anticancer effect. NE prepared using oleic acid as oil and TPGS as a surfactant is an excellent tool for enhancing the solubility of hydrophobic drugs. Increasing the homogenization speed led to a significant effect of decreasing particle size. While increasing the homogenization time decreased NE particle size and increased the contact time between drug and NE components, EE% could be improved. QR-NE is a stable formula that can withstand gravitational and mechanical forces during transportation and handling. The QR-NE showed an excellent release rate compared to the free QR release. Using TPGS in NE produces uniform nanoparticles with no aggregation, and a smooth film around the particles improves the used drug stability and solubility. The latter could enhance the QR release rate and could protect the drug against gastrointestinal degradation, following which intestinal absorption would be further improved. QR-NE inhibited CRC cell viability in a dose-dependent manner, which was more effective than the drug alone. We also found that the NE significantly enhanced the cellular toxicity efficiency in HT-29 and HCT-116 cancer cell lines, resulting in efficient cell killing compared with free agents.

Author Contributions: Conceptualization, H.A.A.E., and H.O.A.; methodology, H.A.A.E., A.F.A., A.M.A., L.M.Y., M.S.A., M.A.A. and H.O.A.; software, H.A.A.E.; validation, H.A.A.E. and H.O.A.; formal analysis, H.A.A.E. and H.O.A.; investigation, H.O.A.; resources, H.O.A.; data curation, H.A.A.E. and H.O.A.; writing—original draft preparation, H.A.A.E., A.F.A., A.M.A., L.M.Y., M.S.A., M.A.A. and H.O.A.; writing—review and editing, H.A.A.E. and H.O.A.; visualization, H.A.A.E. and H.O.A.; supervision, H.A.A.E. and H.O.A.; project administration, H.A.A.E. and H.O.A.; funding acquisition, H.O.A. All authors have read and agreed to the published version of the manuscript.

Funding: His research received no external funding.

Institutional Review Board Statement: The study was conducted according to the guidelines of the Declaration of Helsinki and approved by the Institutional Animal Care and Use Committee at Taif University, Taif, Saudi Arabia. The protocol number is (42-0112).

Informed Consent Statement: Not applicable.

Data Availability Statement: No new data were created or analyzed in this study.

Acknowledgments: Hashem O. Alsaab would like to acknowledge Taif University Researchers. Supporting Project number (TURSP-2020/67), Taif University, Taif, Saudi Arabia.

Conflicts of Interest: The authors declare no conflict of interest.

References

1. Sung, H.; Ferlay, J.; Siegel, R.L.; Laversanne, M.; Soerjomataram, I.; Jemal, A.; Bray, F. Global cancer statistics 2020: GLOBOCAN estimates of incidence and mortality worldwide for 36 cancers in 185 countries. *CA Cancer J. Clin.* **2021**, *71*, 209–249. [CrossRef] [PubMed]
2. Gokhale, J.P.; Mahajan, H.S.; Surana, S.J. Quercetin loaded nanoemulsion-based gel for rheumatoid arthritis: In vivo and in vitro studies. *Biomed. Pharmacother.* **2019**, *112*, 108622. [CrossRef] [PubMed]
3. Fedewa, S.A.; Flanders, W.D.; Ward, K.C.; Lin, C.C.; Jemal, A.; Goding Sauer, A.; Doubeni, C.A.; Goodman, M. Racial and ethnic disparities in interval colorectal cancer incidence: A population-based cohort study. *Ann. Intern. Med.* **2017**, *166*, 857–866. [CrossRef] [PubMed]
4. US Cancer Statistics Working Group. *United States Cancer Statistics: 1999–2014 Incidence and Mortality Web-based Report*; US Department of Health and Human Services, Centers for Disease Control and Prevention and National Cancer Institute: Atlanta, GA, USA, 2017.
5. Bhise, K.; Sau, S.; Alsaab, H.; Kashaw, S.K.; Tekade, R.K.; Iyer, A.K. Nanomedicine for cancer diagnosis and therapy: Advancement, success and structure–activity relationship. *Ther. Deliv.* **2017**, *8*, 1003–1018. [CrossRef]
6. Hussain, Z.; Arooj, M.; Malik, A.; Hussain, F.; Safdar, H.; Khan, S.; Sohail, M.; Pandey, M.; Choudhury, H.; Ei Thu, H. Nanomedicines as emerging platform for simultaneous delivery of cancer therapeutics: New developments in overcoming drug resistance and optimizing anticancer efficacy. *Artif. Cells Nanomed. Biotechnol.* **2018**, *46*, 1015–1024. [CrossRef]
7. Sau, S.; Alsaab, H.O.; Bhise, K.; Alzhrani, R.; Nabil, G.; Iyer, A.K. Multifunctional nanoparticles for cancer immunotherapy: A groundbreaking approach for reprogramming malfunctioned tumor environment. *J. Control. Release* **2018**, *274*, 24–34. [CrossRef]
8. Anitha, A.; Maya, S.; Sivaram, A.J.; Mony, U.; Jayakumar, R. Combinatorial nanomedicines for colon cancer therapy. *Wiley Interdiscip. Rev. Nanomed. Nanobiotechnol.* **2016**, *8*, 151–159. [CrossRef]
9. Pellino, G.; Gallo, G.; Pallante, P.; Capasso, R.; De Stefano, A.; Maretto, I.; Malapelle, U.; Qiu, S.; Nikolaou, S.; Barina, A.; et al. Noninvasive biomarkers of colorectal cancer: Role in diagnosis and personalised treatment perspectives. *Gastroenterol. Res. Pract.* **2018**, *2018*, 2397863. [CrossRef]
10. Bennie, L.A.; McCarthy, H.O.; Coulter, J.A. Enhanced nanoparticle delivery exploiting tumour-responsive formulations. *Cancer Nanotechnol.* **2018**, *9*, 10. [CrossRef]
11. Iyer, A.K.; Khaled, G.; Fang, J.; Maeda, H. Exploiting the enhanced permeability and retention effect for tumor targeting. *Drug Discov. Today* **2006**, *11*, 812–818. [CrossRef]
12. Balasubramanian, V.; Liu, Z.; Hirvonen, J.; Santos, H.A. Bridging the knowledge of different worlds to understand the big picture of cancer nanomedicines. *Adv. Healthc. Mater.* **2018**, *7*, 1700432. [CrossRef] [PubMed]
13. Subhadarshini, S.; Merchant, N.; Raju, G.S.R. Nanomaterials: Diagnosis and Therapeutic Properties. In *Role of Tyrosine Kinases in Gastrointestinal Malignancies*; Springer: Berlin/Heidelberg, Germany, 2018; pp. 235–241.
14. Yoo, J.; Park, C.; Yi, G.; Lee, D.; Koo, H. Active targeting strategies using biological ligands for nanoparticle drug delivery systems. *Cancers* **2019**, *11*, 640. [CrossRef] [PubMed]
15. Gué, E.; Since, M.; Ropars, S.; Herbinet, R.; Le Pluart, L.; Malzert-Fréon, A. Evaluation of the versatile character of a nanoemulsion formulation. *Int. J. Pharm.* **2016**, *498*, 49–65. [CrossRef] [PubMed]
16. Kang, L.; Gao, Z.; Huang, W.; Jin, M.; Wang, Q. Nanocarrier-mediated co-delivery of chemotherapeutic drugs and gene agents for cancer treatment. *Acta Pharm. Sin. B* **2015**, *5*, 169–175. [CrossRef] [PubMed]
17. Sahu, P.; Das, D.; Mishra, V.K.; Kashaw, V.; Kashaw, S.K. Nanoemulsion: A novel eon in cancer chemotherapy. *Mini Rev. Med. Chem.* **2017**, *17*, 1778–1792. [CrossRef]
18. Park, J.B. Flavonoids are potential inhibitors of glucose uptake in U937 cells. *Biochem. Biophys. Res. Commun.* **1999**, *260*, 568–574. [CrossRef]
19. Tang, S.-M.; Deng, X.-T.; Zhou, J.; Li, Q.-P.; Ge, X.-X.; Miao, L. Pharmacological basis and new insights of quercetin action in respect to its anti-cancer effects. *Biomed. Pharmacother.* **2020**, *121*, 109604. [CrossRef]
20. Ghobrial, I.M.; Witzig, T.E.; Adjei, A.A. Targeting apoptosis pathways in cancer therapy. *CA A Cancer J. Clin.* **2005**, *55*, 178–194. [CrossRef]

21. Barbosa, A.I.; Costa Lima, S.A.; Reis, S. Application of pH-responsive fucoidan/chitosan nanoparticles to improve oral quercetin delivery. *Molecules* **2019**, *24*, 346. [CrossRef]
22. Bu, H.; He, X.; Zhang, Z.; Yin, Q.; Yu, H.; Li, Y. A TPGS-incorporating nanoemulsion of paclitaxel circumvents drug resistance in breast cancer. *Int. J. Pharm.* **2014**, *471*, 206–213. [CrossRef]
23. Sharma, S.; Sahni, J.K.; Ali, J.; Baboota, S. Effect of high-pressure homogenization on formulation of TPGS loaded nanoemulsion of rutin–pharmacodynamic and antioxidant studies. *Drug Deliv.* **2015**, *22*, 541–551. [CrossRef] [PubMed]
24. Sessa, M.; Balestrieri, M.L.; Ferrari, G.; Servillo, L.; Castaldo, D.; D'Onofrio, N.; Donsì, F.; Tsao, R. Bioavailability of encapsulated resveratrol into nanoemulsion-based delivery systems. *Food Chem.* **2014**, *147*, 42–50. [CrossRef] [PubMed]
25. El-Enin, H.A.; Al-Shanbari, A.H. Nanostructured liquid crystalline formulation as a remarkable new drug delivery system of anti-epileptic drugs for treating children patients. *Saudi Pharm. J.* **2018**, *26*, 790–800. [CrossRef] [PubMed]
26. Ren, Y.; Li, X.; Han, B.; Zhao, N.; Mu, M.; Wang, C.; Du, Y.; Wang, Y.; Tong, A.; Liu, Y.; et al. Improved anti-colorectal carcinomatosis effect of tannic acid co-loaded with oxaliplatin in nanoparticles encapsulated in thermosensitive hydrogel. *Eur. J. Pharm. Sci.* **2019**, *128*, 279–289. [CrossRef]
27. Riquelme, N.; Zúñiga, R.; Arancibia, C. Physical stability of nanoemulsions with emulsifier mixtures: Replacement of tween 80 with quillaja saponin. *LWT* **2019**, *111*, 760–766. [CrossRef]
28. Ha, J.-W.; Yang, S.-M. Rheological responses of oil-in-oil emulsions in an electric field. *J. Rheol.* **2000**, *44*, 235–256. [CrossRef]
29. Panapisal, V. Effects of surfactant mixture ratio and concentration on nanoemulsion physical stability. *Thai J. Pharm. Sci.* **2016**, *40*, 45–48.
30. Pangeni, R.; Choi, S.W.; Jeon, O.-C.; Byun, Y.; Park, J.W. Multiple nanoemulsion system for an oral combinational delivery of oxaliplatin and 5-fluorouracil: Preparation and in vivo evaluation. *Int. J. Nanomed.* **2016**, *11*, 6379–6399. [CrossRef]
31. Galaup, A.; Opolon, P.; Bouquet, C.; Li, H.; Opolon, D.; Bissery, M.-C.; Tursz, T.; Perricaudet, M.; Griscelli, F. Combined effects of docetaxel and angiostatin gene therapy in prostate tumor model. *Mol. Ther.* **2003**, *7*, 731–740. [CrossRef]
32. Nesamony, J.; Kalra, A.; Majrad, M.S.; Boddu, S.H.S.; Jung, R.; Williams, F.E.; Schnapp, A.M.; Nauli, S.M.; Kalinoski, A.L. Development and characterization of nanostructured mists with potential for actively targeting poorly water-soluble compounds into the lungs. *Pharm. Res.* **2013**, *30*, 2625–2639. [CrossRef]
33. Jafari, S.M.; Assadpoor, E.; He, Y.; Bhandari, B. Re-coalescence of emulsion droplets during high-energy emulsification. *Food Hydrocoll.* **2008**, *22*, 1191–1202. [CrossRef]
34. Bei, D.; Marszalek, J.; Youan, B.-B.C. Formulation of dacarbazine-loaded cubosomes—part I: Influence of formulation variables. *Aaps PharmScitech* **2009**, *10*, 1032–1039. [CrossRef] [PubMed]
35. Iqbal, R.; Mehmood, Z.; Baig, A.; Khalid, N. Formulation and characterization of food grade O/W nanoemulsions encapsulating quercetin and curcumin: Insights on enhancing solubility characteristics. *Food Bioprod. Process.* **2020**, *123*, 304–311. [CrossRef]
36. Pillay, V.; Fassihi, R. In vitro release modulation from crosslinked pellets for site-specific drug delivery to the gastrointestinal tract: I. Comparison of pH-responsive drug release and associated kinetics. *J. Control. Release* **1999**, *59*, 229–242. [CrossRef]
37. Jadhav, C.; Kate, V.; Payghan, S.A. Investigation of effect of non-ionic surfactant on preparation of griseofulvin non-aqueous nanoemulsion. *J. Nanostructure Chem.* **2015**, *5*, 107–113. [CrossRef]
38. Alsaab, H.O.; Sau, S.; Alzhrani, R.M.; Cheriyan, V.T.; Polin, L.A.; Vaishampayan, U.; Rishi, A.K.; Iyer, A.K. Tumor hypoxia directed multimodal nanotherapy for overcoming drug resistance in renal cell carcinoma and reprogramming macrophages. *Biomaterials* **2018**, *183*, 280–294. [CrossRef]
39. Cheriyan, V.T.; Alsaab, H.O.; Sekhar, S.; Stieber, C.; Kesharwani, P.; Sau, S.; Muthu, M.; Polin, L.A.; Levi, E.; Iyer, A.K.; et al. A CARP-1 functional mimetic loaded vitamin E-TPGS micellar nano-formulation for inhibition of renal cell carcinoma. *Oncotarget* **2017**, *8*, 104928–104945. [CrossRef]
40. Buyukozturk, F.; Benneyan, J.C.; Carrier, R.L. Impact of emulsion-based drug delivery systems on intestinal permeability and drug release kinetics. *J. Control. Release* **2010**, *142*, 22–30. [CrossRef]
41. Md, S.; Alhakamy, N.A.; Aldawsari, H.M.; Husain, M.; Kotta, S.; Abdullah, S.T.; A Fahmy, U.; Alfaleh, M.A.; Asfour, H.Z. Formulation design, statistical optimization, and in vitro evaluation of a naringenin nanoemulsion to enhance apoptotic activity in A549 lung cancer cells. *Pharmaceuticals* **2020**, *13*, 152. [CrossRef]